

Evaluation of the Inhibition Effect of Some Novel Organic Compounds (phenol derivatives) for Corrosion of α -brass in Acid Solutions

A. S. Fouda^{1,*}, F. M. El-Taweel², N. H. Mohamed¹

¹ Department of Chemistry, Faculty of Science, El-Mansoura University, El-Mansoura-35516, Egypt,

² Department of Chemistry, Faculty of Science, Damietta University

*E-mail: asfouda@hotmail.com, asfouda@mans.edu.eg

Received: 5 September 2019 / Accepted: 11 October 2019 / Published: 30 November 2019

The influence of the addition of some organic compounds (OCs) on the corrosion of α -brass immersed in 1M HNO₃ were studied. Gravimetric and electrochemical (AC impedance (EIS), electrochemical frequency modulation (EFM) and polarization (PP)) tests were used separately for the experimental investigation. The protection efficiency of organic inhibitors improves with a rise in concentration and the temperature range from 25°C to 50°C. PP tests also designated that organic inhibitors acted as mixed-kind inhibitors. Surface investigation utilized atomic force microscope (AFM) displays an important morphological development on the α -brass surface with the adding of the inhibitor. Adsorption isotherm showed that inhibitor protection mechanism followed the Langmuir isotherm model. Correlation among protection efficiencies and molecular orbital energy was a study of Density functional theory (DFT).

Keywords: α -Brass corrosion, HNO₃, Organic compounds, PP, EFM, EIS

1. INTRODUCTION

In terms of wider use and versatility in industrial and services application, the copper and α -brass are of significant importance in material's selection consideration for corrosion and protection in corrosive environments [1-2]. HNO₃ is an oxidizing agent rely on its concentration. HNO₃ reacts with metals by obtaining the metal nitrates and hydrogen [3]. It is recognized [4] that most of the base metals react with HNO₃ to obtain hydrogen rich compound (NH₂OH or NH₃), whereas noble metals like copper or silver yield compound rich in oxygen (NO, NO₂ and HNO₂). The impact of inhibitors is often linked with adsorption chemical or physical. This phenomenon had been linked with N, S, O, and multiple bonds or aromatic rings in the inhibitor that were presented as hetero atoms that adsorbed on the surface of metal [5]. For example, the protection enactment of these aligning derivatives had examined as eco-

friendly corrosion protection for brass in 1 M HNO₃ [6]. Other researches designated that organic compounds have been renowned as remarkably effective protection of brasses and copper [7–8].

The choice of these compounds is constructed on: a) are extremely soluble in the test solution, and b) contain polar functional groups (such as CN, N=N and –C=O) and aromatic moiety which adsorbed on the brass surface.

The aim of the present paper describes corrosion of commercial 60/40 α -brass in 1 M HNO₃ solutions by some phenol derivatives as inhibitors. Further, theoretical chemical approaches have used to corroborate the experimental findings.

2. MATERIALS AND TECHNIQUES

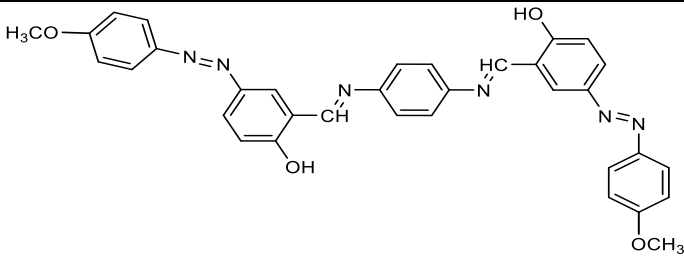
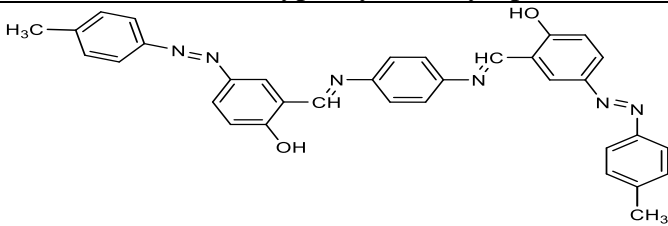
2.1. Materials

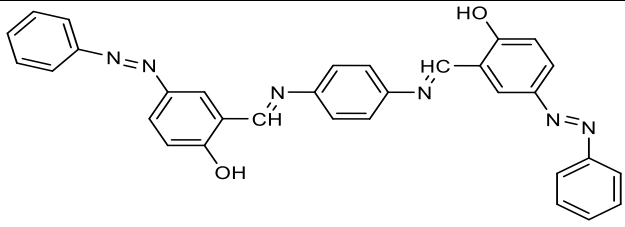
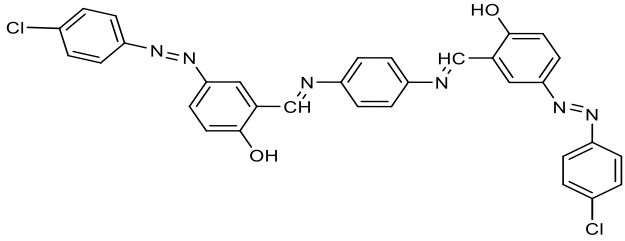
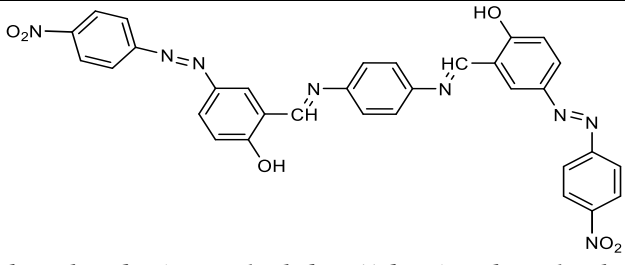
The tests have achieved by local commercial α -brass (Helwan Company of Industries Non-Ferrous, Egypt) with this conformation (weight %) Cu 63 Brass 37

2.2. Preparation of the compounds acting as inhibitors

The inhibitors used were selected from phenol derivatives and displayed in the below Table 1. These derivatives were synthesized and characterized as before [9].

Table 1. Show the chemical structure and molecular formulas of the studied compounds

Compound	Structures, Names	Mol. Formulas, Mol. Weights
A	 <p>2,2'-((1,4-phenylenebis (azan-1-ylidene)) bis(methan-1-yl-ylidene)) bis(4-(4- methoxyphenyldiazenyl) phenol)</p>	<p>C₃₄H₂₈N₆O₄ 584.62</p>
B	 <p>2,2'-((1,4-phenylenebis (azan-1-ylidene)) bis(methan-1-yl-ylidene)) bis(4-(p-tolyldiazenyl)phenol)</p>	<p>C₃₄H₂₈N₆O₂ 552.64</p>

C	 <p><i>2,2'-((1,4- phenylenebis (azan-1-ylidene)) bis (methan-1-yl-ylidene)) bis (4-(phenyldiazenyl)phenol)</i></p>	$C_{32}H_{24}N_6O_2$ 524.58
D	 <p><i>2,2'-((1,4- phenylenebis(azan-1-ylidene)) bis (methan-1-yl-ylidene)) bis (4-(4-chlorophenyldiazenyl) phenol)</i></p>	$C_{32}H_{22}Cl_{12}N_6O_2$ 593.47
E	 <p><i>2,2'-((1,4- phenylenebis(azan-1-ylidene)) bis (methan-1-yl-ylidene)) bis (4-(4-nitrophenyldiazenyl) phenol)</i></p>	$C_{32}H_{22}N_8O_6$ 614.17

2.3. Chemicals and solutions

The electrochemical tests utilized electrode working (anode) which made from α -brass coins. The corrosive solution applied (1 M HNO_3) was prepared by dilution of analytical grade, 67% HNO_3 by using bidistilled water and we checked its concentration by titration with standardized NaOH. We calculated the weight of each inhibitor, dissolved by DMF then with ethyl alcohol and prepared the wanted concentrations by dilution with bidistilled water. The concentration range was (5×10^{-6} - 21×10^{-6} M). The OCs that employed as a part of this paper had listed in Table1.

2.4. Tests used for corrosion estimations

2.4.1. Weight reduction (WR) test

WR tests were utilized square coins of size $20 \times 20 \times 2$ mm, prior to all tests, the brass samples were ground with different emery papers (400, 800 and 1500 grit size), washed carefully with acetone and bidistilled water and dried. The WR test was put in a 100 ml capability glass beaker contain 100 ml of 1M HNO_3 with and without various concentrations of examining compounds. All the corrosive tests were air opened, splashed, dried, and weighed exactly. The normal WR of the brass sheets could be obtained. The % IE and the θ were computed as in equation (1)

$$\% \text{ IE} = 100 \times \theta = 100 \times [(W^{\circ} - W)/W^{\circ}] \quad (1)$$

Where W° and W are the values of the average WR in the absence and presence of the compound, correspondingly.

2.4.2. Potentiodynamic polarization technique

The electrochemical techniques have performed using PCI4-G750 Potentiostat/Galvanostat and a personal computer with Gamry software Echem 5.2 for measurements. The utilized electrical circuit include of three electrodes (SCE reference electrode, Pt auxiliary electrode and brass electrode). 1 cm² of the brass electrode is ready, and cleaned as illustrated in WR test. All electrochemical studies were performed at 25 ± 1 °C. (PP) is a beneficial method due to they give more information about the corrosion protection and the factors influence the corrosion process and hindrance behavior of the OCs. This is done by determining the potential- current plots of the α -brass / solution system. In PP test, electrode potential from –1000 to 1000 mV was applied at scanning rate 1 mVs⁻¹.

2.4.3. EIS technique

The frequency range is between 100 kHz and 0.1 Hz and AC signal is 10 mV peak to peak. % IE and θ were obtained by employing the next relation [10]:

$$\% \text{ IE} = 100 \times \theta = 100 \times [1 - (R^{\circ}_{ct} / R_{ct})] \quad (2)$$

Where R°_{ct} and R_{ct} are the resistances without and with inhibitor, separately

2.4.4-EFM technique

EFM tests reached by the decision for the frequencies of range 2 and 5Hz be influenced by on three arguments [11]. The higher peaks have applied to given i_{corr} , (CF-2 & CF-3) and (β_c & β_a) [12].

2.4.5. Surface morphology

For surface morphology, the brass coins putted to the test solutions for 24 hours. AFM test utilized to measure the roughness value from various surfaces of α -brass [13]. AFM device model is a Pico SPM2100.

3. RESULTS AND DISCUSSION

3.1. PP estimations

Theoretically, brass can hardly be corroded in the deoxygenated aggressive solution, as brass can't liberate hydrogen from corrosive measures giving to the principles of chemical thermodynamics [14]. Figure 1 displays the PP performance of α -brass in 1M HNO₃ in the presence and absence of various concentrations of OCs (A). Similar curves have received for other compounds (not displayed).

The obtained parameters such as (i_{corr}), (E_{corr}), (β_c), (β_a), (θ) and (% IE) were measured from the curves of (Figure 1) and recorded in (Table 2) for all OCs. Table 2 displayed that both the anodic and cathodic responses is influence by the adding of OCs and the rise protection efficiency as the OCs concentration improves, showing that OCs act as mixed-kind inhibitors in 1M HNO₃. i_{corr} decreases clearly after the addition of OCs in 1M HNO₃ and % IE improve with increase the OCs concentration and measured from equation (3):

$$\% \text{ IE} = [(i_{\text{corr}} - i_{\text{corr(inh)}}) / i_{\text{corr}}] \times 100 \quad (3)$$

Where i_{corr} and $i_{\text{corr(inh)}}$ are the unprotected and protected current data, correspondingly. The IE of the OCs is detected to be: A > B > C > D > E.

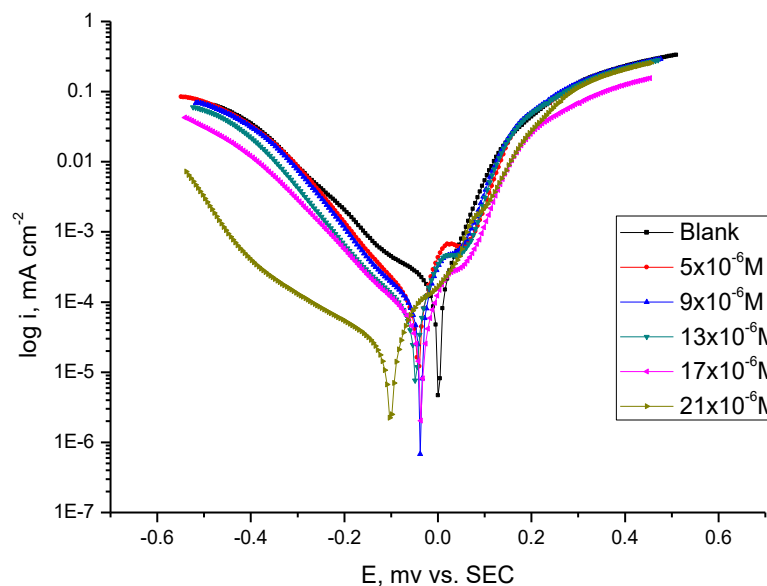


Figure 1. PP plots for α -brass corrosion with and without different concentrations of inhibitor (A) at 25°C

Table 2. PP data of α -brass in 1M HNO₃ include different concentrations of OCs at 25°C

Comp	Conc., $\times 10^{-6}$ M 10^6 M	i_{corr} , $\mu\text{A cm}^{-2}$	$-E_{\text{corr}}$, mV vs SCE	β_a , mV dec ⁻¹	β_c , mV dec ⁻¹	C.R mpy	θ	% IE
Blank	0.0	504	33	71	154	243.5		
A	5	102	43	106	136	49.4	0.798	79.8
	9	65.8	38	80	128	31.8	0.869	86.9
	13	61.1	47	94	141	29.5	0.879	87.9
	17	49.5	36	95	151	23.9	0.902	90.2
	21	30.2	10	97	135	14.6	0.940	94.0
B	5	375	56	79	152	181.5	0.256	25.6
	9	284	43	86	163	137.5	0.436	43.6
	13	224	25	79	159	108.2	0.555	55.5
	17	77.6	10	78	148	37.5	0.846	84.6
	21	60.1	30	68	138	29.6	0.881	88.1
	5	249	47	94	151	120.3	0.506	50.6

C	9	235	25	99	181	113.5	0.534	53.4
	13	213	10	82	141	102.8	0.577	57.7
	17	167	37	97	166	80.9	0.669	66.9
	21	62.6	59	93	155	30.2	0.8756	87.6
D	5	401	41	85	162	193.7	0.204	20.4
	9	222	19	97	121	107.1	0.559	55.9
	13	138	18	76	138	66.5	0.726	72.6
	17	85	17	96	189	41.3	0.831	83.1
	21	65.4	28	91	184	31.6	0.870	87.0
E	5	367	15	82	143	177.3	0.272	27.2
	9	334	44	95	170	161.6	0.337	33.7
	13	314	59	83	160	151.7	0.377	37.7
	17	240	14	91	161	116.1	0.524	52.4
	21	96	22	94	154	46.4	0.809	80.9

3.2. EIS measurements

Figure 2 shows the Nyquist and Bode plots obtained for the brass electrode at corresponding corrosion potentials after half hours immersion in 1M HNO₃ without and with various concentrations of the compound (A) at 25°C.

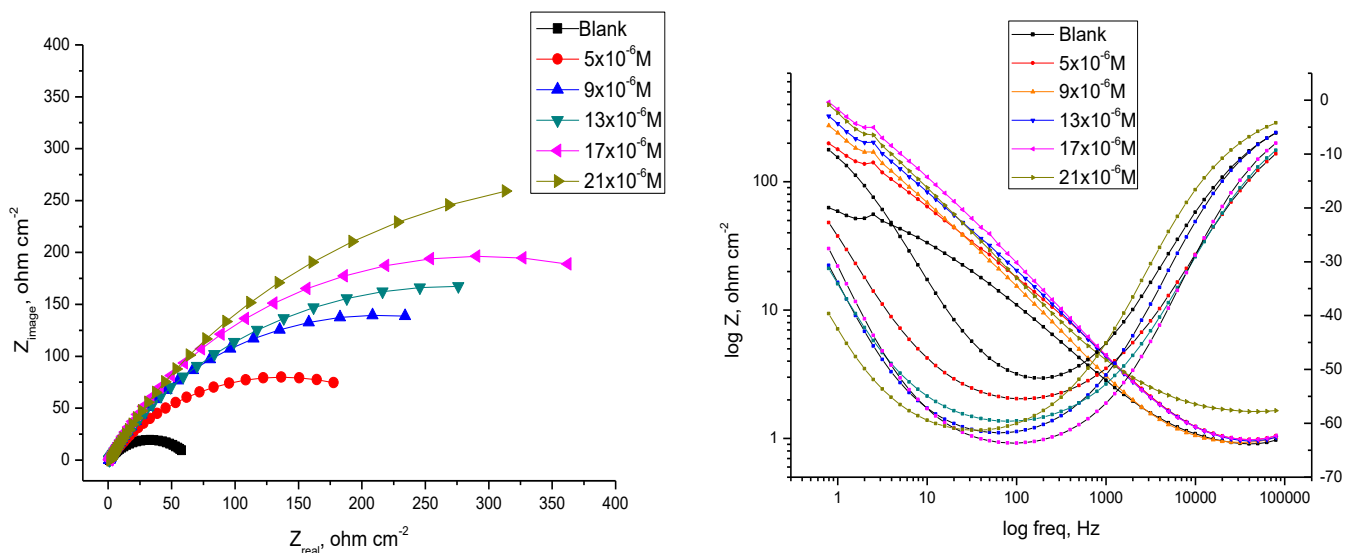


Figure 2. EIS Bode and Nyquist plans for Brass in 1M HNO₃ in the presence and absence of various concentrations of compound (A) 25°C

The same curves were obtained for OCs (not displayed). As the OCs concentration increases, the semi-circle diameter increases. EIS data of the OCs were analyzed utilizing the circuit equivalent, Figure 3, which fits well with our outcome data [15,16]. The double layer capacitance, C_{dl} , for a circuit containing a CPE value (Y^0 and n) were measured from eq. (4) [17]:

$$C_{dl} = Y^0 \omega^{n-1} / \sin [n (\pi / 2)] \quad (4)$$

Where $\omega = 2\pi f_{\max}$, f_{\max} is the frequency maximum. The diameter semi-circle dealings the charge transfer resistance, R_{ct} , and inversely proportional to the i_{corr} data. Improve in R_{ct} led to rise in the width of the double layer that OCs adsorbed [18]. In adding, the (C_{dl}) value lowered by counting OCs into corrosive solution. Also, C_{dl} can be measured by the next equation [19]:

$$C_{dl} = \epsilon\epsilon_0 (A/\delta) \quad (5)$$

C_{dl} lowered due to the exchange of the adsorbed water molecules at the α -brass surface by the OCs molecules having lower dielectric constant [19]. The EIS data were listed in Table 3.

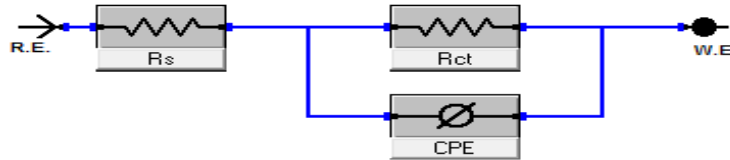


Figure 3. Equivalent circuit obtained to model EIS values in 1M HNO_3

Table 3. Data obtained from EIS for α -brass in 1M HNO_3 with and without various concentrations of OCs at 25°C

Comp	Conc., x 10^{-6} M	R_{ct} , $\Omega \text{ cm}^2$	C_{dl} , $\times 10^{-10} \mu\text{F cm}^{-2}$	θ	%IE
Blank	0	55.7	2.31	--	--
A	5	272.9	3.73	0.796	79.6
	9	428.4	3.95	0.87	87.0
	13	540.7	3.56	0.897	89.7
	17	587	2.21	0.905	90.5
	21	841.5	3.98	0.934	93.4
B	5	94.95	3.29	0.413	41.3
	9	174.7	3.26	0.681	68.1
	13	249.8	3.04	0.777	77.7
	17	527.7	2.48	0.894	89.4
	21	746.4	1.35	0.925	92.5
C	5	74.63	2.78	0.253	25.3
	9	158.6	2.45	0.648	64.8
	13	228.7	2	0.756	75.6
	17	425.1	1.96	0.869	86.9
	21	624.2	1.6	0.911	91.1
D	5	68.96	3.93	0.191	19.1
	9	124.9	2.97	0.554	55.4
	13	208.5	2.38	0.733	73.3
	17	237.2	1.88	0.765	76.5
	21	426.1	1.43	0.869	86.9
E	5	62.1	3.33	0.102	10.2
	9	102.5	2.82	0.456	45.6
	13	183.5	2.65	0.696	69.6
	17	193.5	2.53	0.712	71.2
	21	341.7	2.33	0.837	83.7

3.3. EFM measurements

EFM for α -brass electrode in aggressive medium in presence and absence of various concentrations of compound (A) was drawn in Figure 4. Similar intermodulation spectra were obtained for various OCs (not displayed). Data obtained from EFM were recorded in Table 4. It is observed that i_{corr} lowered by raising the OCs concentration. Also, CF-2 and CF-3 values were very approach to theoretical data and this agrees with the EFM theory [20]. The % IE were computed from EFM is in the direction: $A > B > C > D > E$

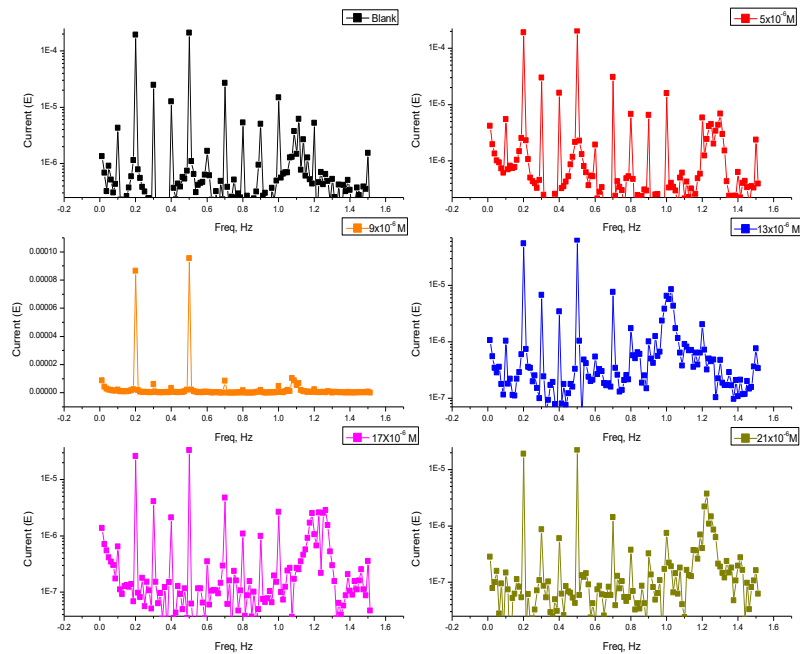


Figure 4. EFM spectra for α -brass in corrosive solution without and with different concentrations compound (A) at 25°C

Table 4. Data obtained by EFM tests for brass without and with various concentrations of OCs in 1M HNO_3 at 25°C

Comp	Conc., x 10^{-6} M	i_{corr} , μAcm^{-2}	β_a , mVdec^{-1}	β_c , mVdec^{-1}	C.R, mpy	CF-2	CF-3	θ	%IE
Blank	0.0	262.3	63	127	126.8	1.9	3.1	-----	-----
A	5	234.3	56	122	113.3	1.9	2.9	0.107	10.7
	9	113.4	67	102	54.8	1.8	2.9	0.92	92.0
	13	77.3	64	122	37.3	1.9	2.9	0.705	70.5
	17	34.2	56	114	16.4	1.9	2.7	0.870	87.0
	21	31.1	84	117	15.1	1.7	3.4	0.881	88.1
B	5	189.9	67	109	91.8	1.8	3.2	0.276	27.6
	9	106.6	69	106	51.5	1.7	2.9	0.593	59.3
	13	90.6	80	109	46.8	1.8	3.2	0.654	65.4
	17	92.3	82	134	44.6	1.9	2.7	0.648	67.8
	21	35.7	82	131	17.3	1.8	2.7	0.864	86.4

C	5	82.4	77	122	39.8	1.9	3.3	0.689	68.9
	9	78.5	78	122	38.1	2.1	3.2	0.700	70.0
	13	50.8	86	118	24.5	1.7	2.6	0.806	80.6
	17	41.6	64	120	20.1	2.2	2.9	0.841	84.1
	21	37.6	81	123	18.2	1.9	2.7	0.863	86.3
D	5	50.2	54	122	24.2	1.8	2.9	0.808	80.8
	9	37.7	78	105	18.2	1.7	3.1	0.856	85.6
	13	33.0	70	120	15.9	1.9	2.9	0.874	87.4
	17	30.97	81	105	14.9	1.9	3.0	0.882	88.2
	21	21.9	41	116	10.6	2.1	3.2	0.828	82.8
E	5	155.5	57	106	75.1	1.9	3.1	0.407	40.7
	9	136.1	62	106	65.8	2.2	2.9	0.481	48.1
	13	114.2	78	121	55.1	1.8	3.1	0.565	56.5
	17	85.0	62	104	41.1	1.9	2.9	0.676	67.6
	21	68.7	77	122	33.2	1.8	2.8	0.738	73.8

3.4. WR measurements

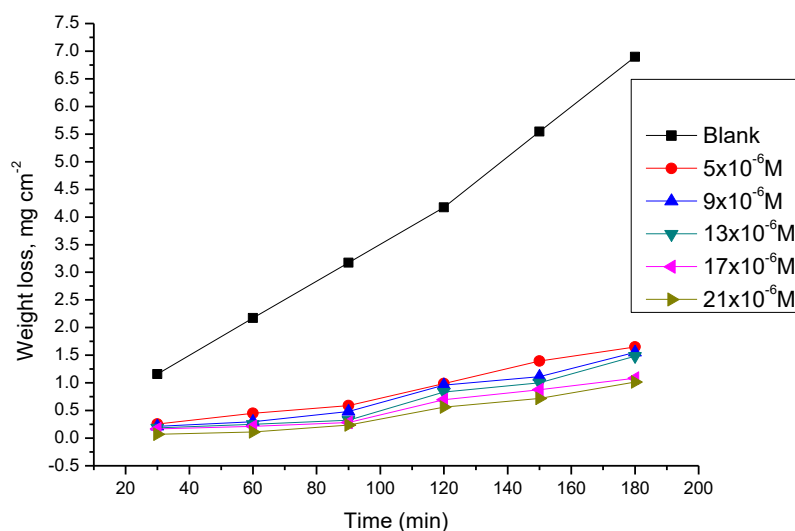


Figure 5. Time-WR curves for the dissolution of α -brass in the presence and absence of various concentrations of the compound (A) at 25°C

Figure 5 demonstrates the curve of WR - time at 25°C for α -brass in aggressive solution with and without various concentrations of a compound (A). Like diagrams obtained from other compounds (not presented). As shown from this Figure, by improving OCs concentration, the WR of α -brass sample lowered. This means that OCs act as inhibitors for α -brass in acid solution. It is also clear that WR was in linear variation with time for unprotected and protected corrosive solution [21]. % IE calculated by OCs lower in the sequence: A > B > C > D > E.

Table 5. % IE of all compounds at 90 min for α -brass corrosion in 1M HNO₃ solution in the absence and presence of various concentrations of OCs as measured from WR test at 25°C

Comp	A		B		C		D		E	
Conc., x 10 ⁻⁶ M	Θ	% IE	Θ	% IE	Θ	% IE	Θ	% IE	Θ	% IE
5	0.814	81.4	0.771	77.1	0.751	75.1	0.719	71.9	0.624	62.4
9	0.848	84.8	0.781	78.1	0.779	77.9	0.739	73.9	0.711	71.1
13	0.897	89.7	0.81	81	0.793	79.3	0.773	77.3	0.733	73.3
17	0.911	91.1	0.867	86.7	0.821	82.1	0.807	80.7	0.76	76
21	0.925	92.5	0.906	90.6	0.898	89.8	0.843	84.3	0.782	78.2

3.5. Impact of temperature

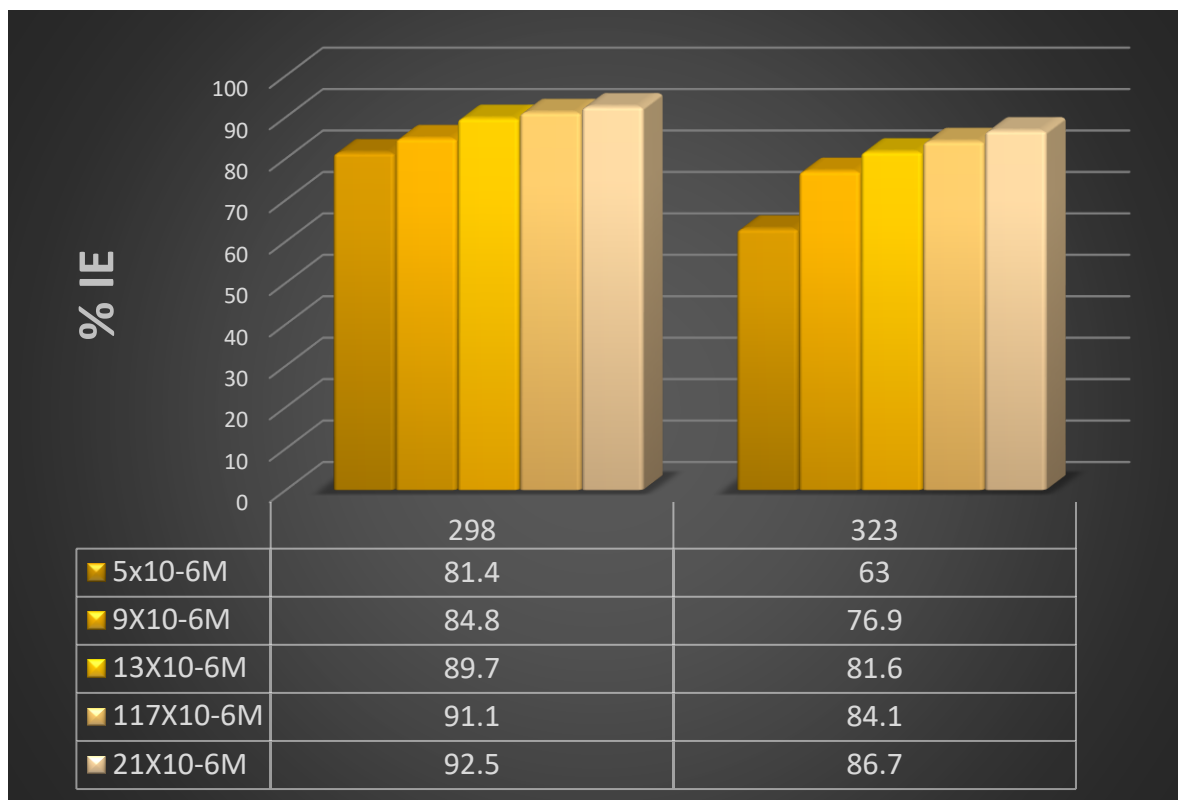
**Figure 6.** Temperature effect on % IE at various concentrations of compound (A) for α -brass dissolution in 1M HNO₃ at different temperatures (298 – 323K)

Figure 6 shows variation of IE of compound (A) with 298 and 323 K using various concentrations of the compound (A) for α -brass corrosion in 1M HNO₃, (alike curves were acquired in presence of the OCs, (but not displayed). The rise of % IE with decreasing the temperature; this means that the inhibitors are present adsorbed physically at low temperatures.

The (E_a^*) utilized by Arrhenius equation (6) [22]:

$$k_{\text{corr}} = A \exp (-E_a^* / RT) \quad (6)$$

Where A is an Arrhenius constant and T is the absolute temperature. The values of E_a^* obtained from (Figure 7) in the presence and absence of OCs at various temperatures are listed in Table 6. The effective E_a^* lead to higher data within the sight of these OCs than without them. E_a^* was improved with the adding of various concentrations of OCs. This will used to raise the energy barrier for the corrosion process. These data show that the existence of OCs improves the E_a^* of α -brass dissolution reaction [23-24]. (ΔH^* , ΔS^*) are measured from transition state equation (7) [25]:

$$k_{\text{corr}} = RT/Nh \exp(\Delta S^*/R) \exp(-\Delta H^*/RT) \quad (7)$$

Figure 8 displays a plot of $(1/T)$ vs. $\log(k_{\text{corr}}/T)$, the data of ΔS^* and ΔH^* are measured and also listed in Table 6. Generally, ΔH^* of a chemisorption manner arrived (100 kJ mol^{-1}) [26-27]. The enthalpy improves in the presence of the OCs, indicating the increase of the height of the energy barrier of the corrosion process to value rely on the concentration of the present compounds. The ΔS^* are -ve data; this display that the activated complex in the rate-determining shows association relatively than dissociation [28].

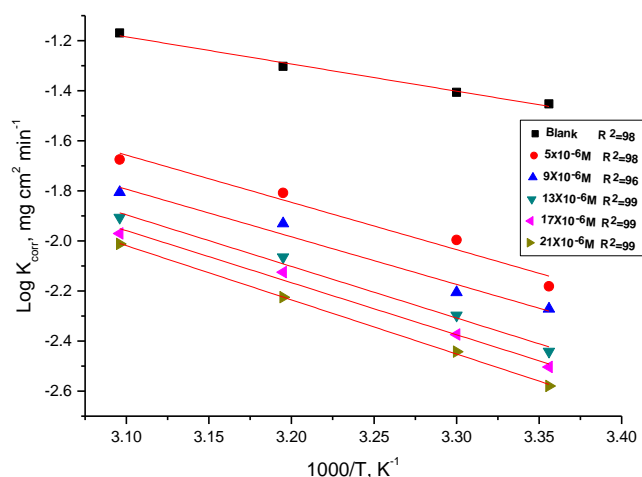


Figure 7. Arrhenius plots for the dissolution of α -brass in 1M HNO_3 for compound (A)

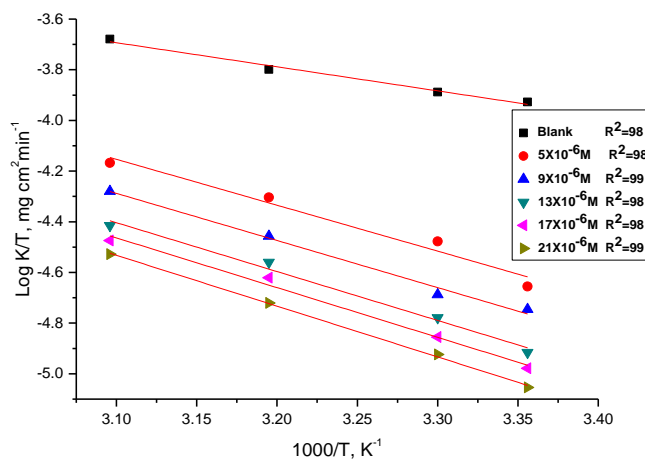


Figure 8. $(\log k_{\text{corr}} / T)$ vs. $1/T$ for the dissolution of α -brass in 1M HNO_3 for compound (A)

Table 6. Activation parameters for α -brass in 1M HNO₃ in presence and absence of different concentrations of OCs

Comp	Conc., x 10 ⁻⁶ M	E _a [*] , kJ mol ⁻¹	ΔH^* , kJ mol ⁻¹	$-\Delta S^*$, J mol ⁻¹ K ⁻¹
Blank	0.0	20.8	7.90	211.8
A	5	36.1	15.1	169.5
	9	36.4	15.4	169.2
	13	39.4	16.0	167.3
	17	39.8	16.3	166.5
	21	41.4	16.6	165.3
B	5	34.5	14.4	169.5
	9	36.1	15.7	169.2
	13	36.4	15.8	167.3
	17	37.1	15.9	166.5
	21	37.8	16.1	165.3
C	5	34.8	15.2	165.4
	9	35.1	15.5	164.6
	13	35.7	15.8	164.0
	17	36.2	16.0	163.5
	21	37.0	16.3	163.1
D	5	33.8	15.2	165.2
	9	34.0	15.5	164.4
	13	34.2	15.6	164.2
	17	34.9	15.7	164.3
	21	35.8	15.9	163.8
E	1	32.1	12.8	181.3
	9	33.3	13.6	177.1
	13	33.7	13.9	175.5
	17	34.2	14.2	174.1
	21	34.6	14.6	173.4

3.7. Adsorption isotherms

Adsorption isotherms are commonly used to recognize the mechanism of protection on the metal surface [29-31]. The excellent fit was obeying Langmuir, which are signified in Figure (9) for compound (A) expressed by:

$$C/\Theta = 1/k_{\text{ads}} + C \quad (8)$$

Where K_{ads} is constant of adsorption equilibrium, the $\Delta G^{\circ}_{\text{ads}}$ can be calculated by

$$\Delta G^{\circ}_{\text{ads}} = -RT \ln (55.5 K_{\text{ads}}) \quad (9)$$

Where 55.5 = molar concentration of water in the solution in M⁻¹. Thermodynamic parameters obtained from adsorption of the OCs on α -brass surface in 1 M HNO₃ at various temperatures were recorded in the Table (7). It was established that $\Delta G^{\circ}_{\text{ads}}$ has –ve value between 40 to 45 kJ mol⁻¹ designating that the OCs adsorption on α -brass in 1 M HNO₃ solution is a spontaneous process belong to chemisorption mechanism [32].

The standard enthalpy $\Delta H^\circ_{\text{ads}}$ and entropy obtained from adsorption $\Delta S^\circ_{\text{ads}}$ can be measured using eq.10&11

$$\ln K_{\text{ads}} = [-\Delta H_{\text{ads}} / RT] + \text{const} \quad (10)$$

$$\Delta S_{\text{ads}} = (\Delta H_{\text{ads}} - \Delta G_{\text{ads}}) / T \quad (11)$$

The value of $\Delta H^\circ_{\text{ads}}$ was evaluated from the slope of the diagrams of $\log K_{\text{ads}}$ versus $1/T$ see Figure 10. The $-ve$ sign data of $\Delta H^\circ_{\text{ads}}$ ensures that the process of adsorption is an exothermic [35-36]. Negative data $\Delta S^\circ_{\text{ads}}$ show that decreasing in the disorder of corrosion procedure on an α -brass surface in 1M HNO_3 utilizing OCs as corrosion protection (Table 7) [37-38].

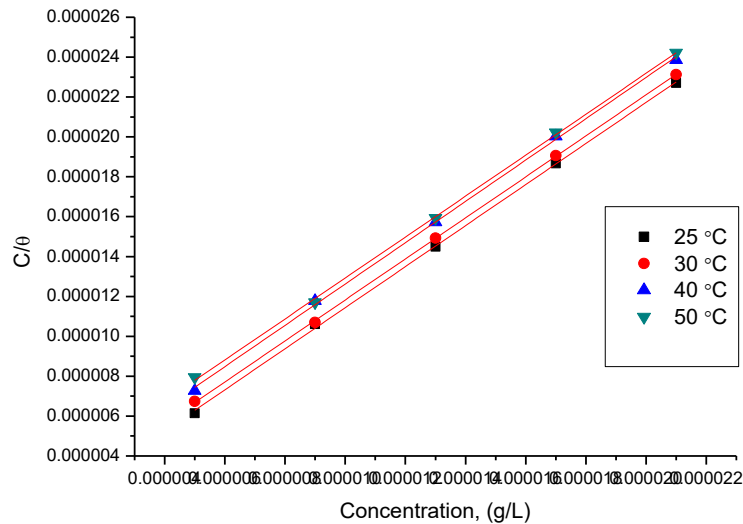


Figure 9. Langmuir adsorption plots for α -brass in 1M HNO_3 at various temperatures

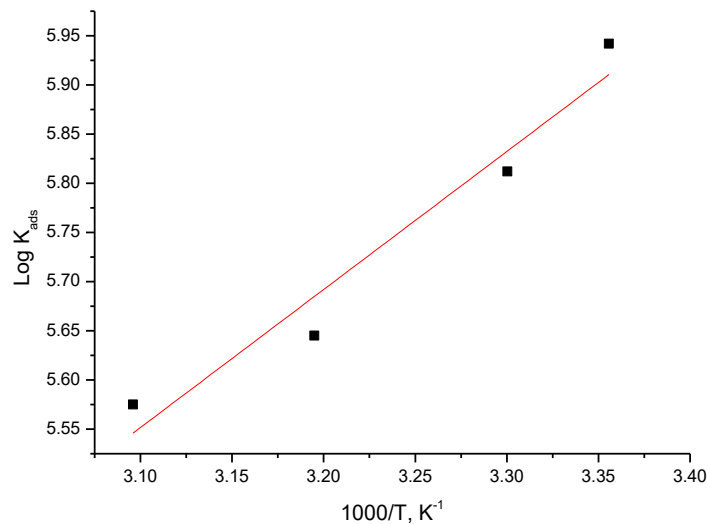


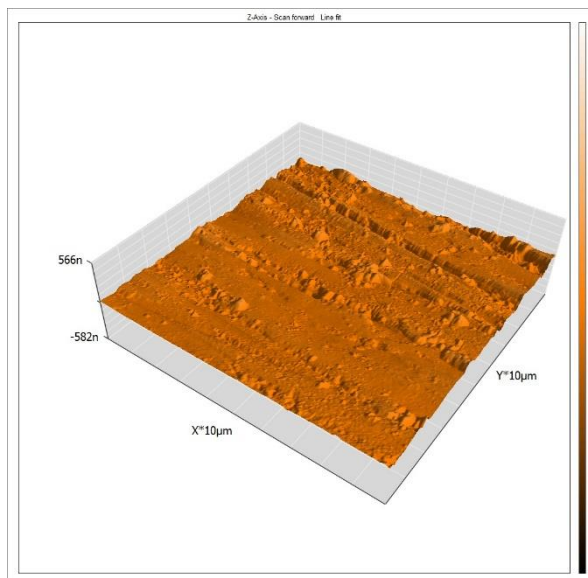
Figure 10. $\log K_{\text{ads}}$ versus $1/T$ for the adsorption of compound (A) in 1M HNO_3

Table 7. Parameters for α -brass 1M HNO₃ for OCs at various temperature

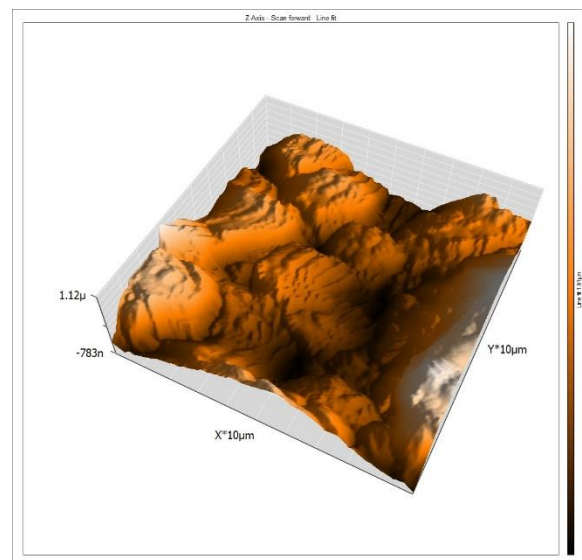
Comp	Temp., K	K _{ads} M ⁻¹	$-\Delta G^{\circ}_{\text{ads}}$ kJ mol ⁻¹	$-\Delta H^{\circ}_{\text{ads}}$ kJ mol ⁻¹	$-\Delta S^{\circ}_{\text{ads}}$ J mol ⁻¹ K ⁻¹
A	298	87.5	43.8	26	147.2
	303	64.9	43.8		144.7
	313	44.2	44.2		141.5
	323	37.6	45.2		140.1
B	298	52.9	42.7	27	143.0
	303	37.9	42.4		140.2
	313	30.0	43.2		138.3
	323	21.2	43.7		135.4
C	298	52.9	42.6	34	142.9
	303	34.2	42.2		139.3
	313	21.5	42.4		135.5
	323	17.6	43.2		133.8
D	298	38.8	41.8	36	140.4
	303	23.2	41.2		136.1
	313	18.0	41.9		134.0
	323	17.4	41.2		133.2
E	298	43.4	41.1	42	140.1
	303	24.4	41.3		135.5
	313	15.7	41.6		132.9
	323	10.7	40.8		129.6

3.8. (AFM) examination

AFM is a remarkable technique used for measuring the surface roughness with high resolution [39]. Many details about α -brass surface morphology can be obtained from AFM measurements that help to explain the corrosion process. The three-dimensional AFM images represented in Fig (11).



Free



Blank

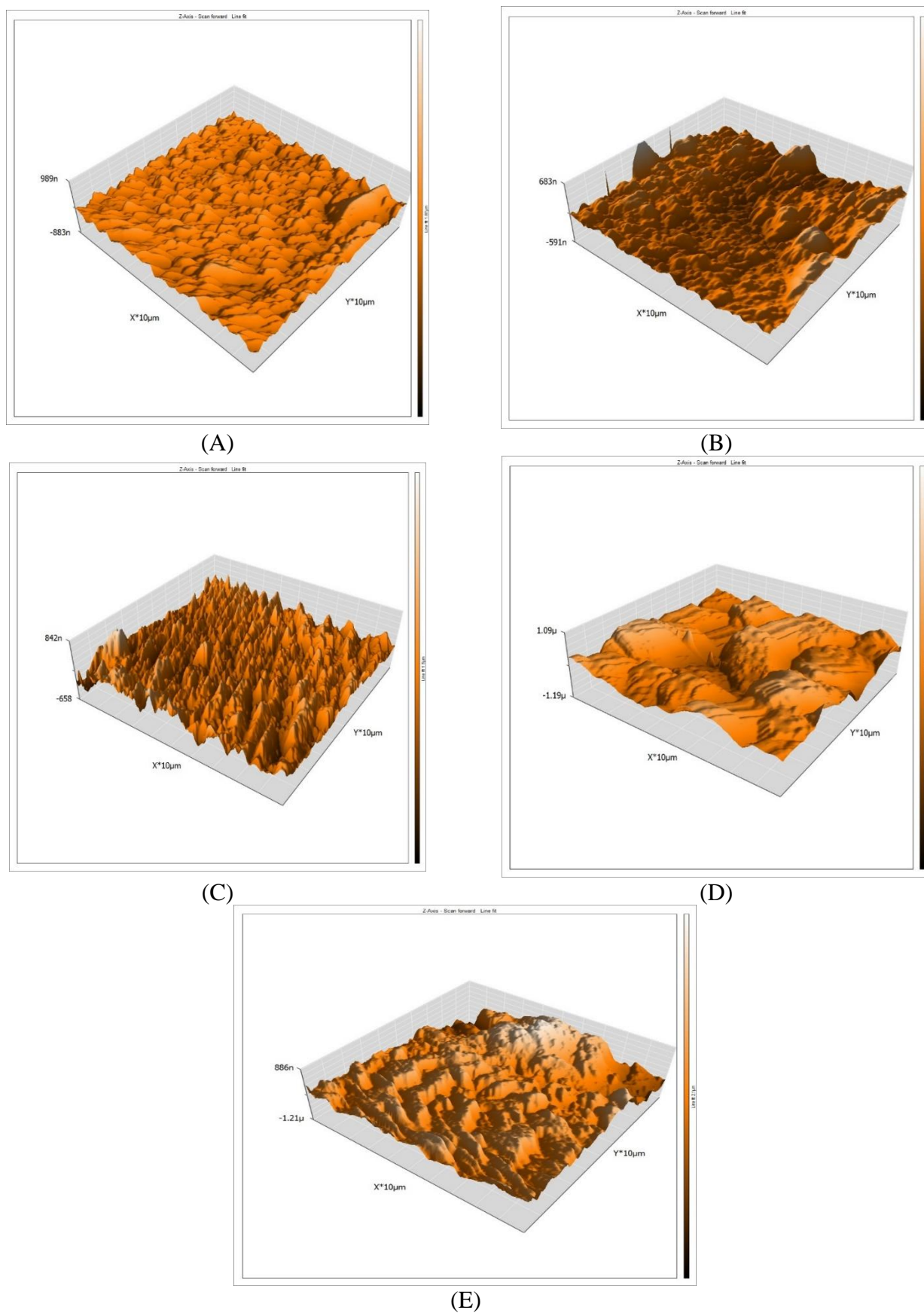


Figure 11. AFM 3D images α -brass, free specimen, with 1.0M HNO_3 for 24 hr and (A-E) with 1M HNO_3 containing OCs for 24 hr

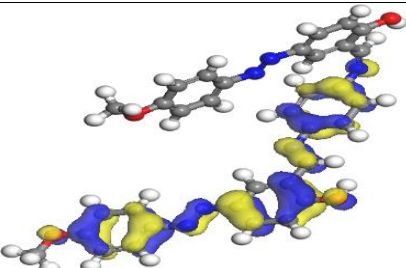
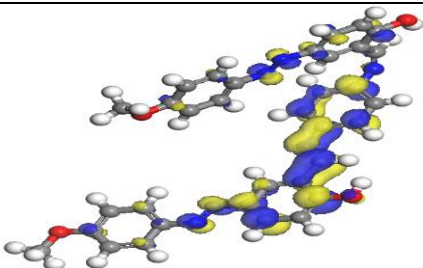
Table 8. AFM data of OCs for 24 hr at 25°C

Coins	Average roughness (S_a) nm
Free	15
Blank	302
(A)	78
(B)	91
(C)	117
(D)	163
(E)	180

The roughness calculated from the AFM image have summarized in Table (8). The values showed that the roughness increases with adding HNO_3 due to the corrosion occurs on the α -brass surface but decreased with adding the prepared [40].

3.9. Theoretical study of inhibitors

Quantum chemical computations are powerful tools commonly applied in studying the corrosion inhibitor effect of OCs in terms of chemical reactivity through interpreting some molecular parameters from the energy. The calculations of quantum had achieved on the neutral and protonated species. (HOMO), and (LUMO) for the protonated form of the furan derivatives investigated are shown in Figure 12 [41-42]. Small ΔE services adsorption of the OCs and thus given greater protection productivity. The (ΔE) increased from (A) to (E). Table 9 and Figure 12 demonstrates the optimized structures of the OCs. Table 9 shows that a compound (A) has the lowered ΔE paralleled with the other OCs. Consequently, compound (A) could be expectable that more disposition to adsorption on the α -brass than the other OCs. It was remarkable that the presence of an electron donating group such as $-OCH_3$ and $-CH_3$, are more preferred than $-Cl$ and $-NO_2$ group to improve the %IE of the OCs. Table 9 displayed that the measured dipole moment improve from ($E > D > C > B > A$).

Inhibitor s	HOMO	LUMO
A		

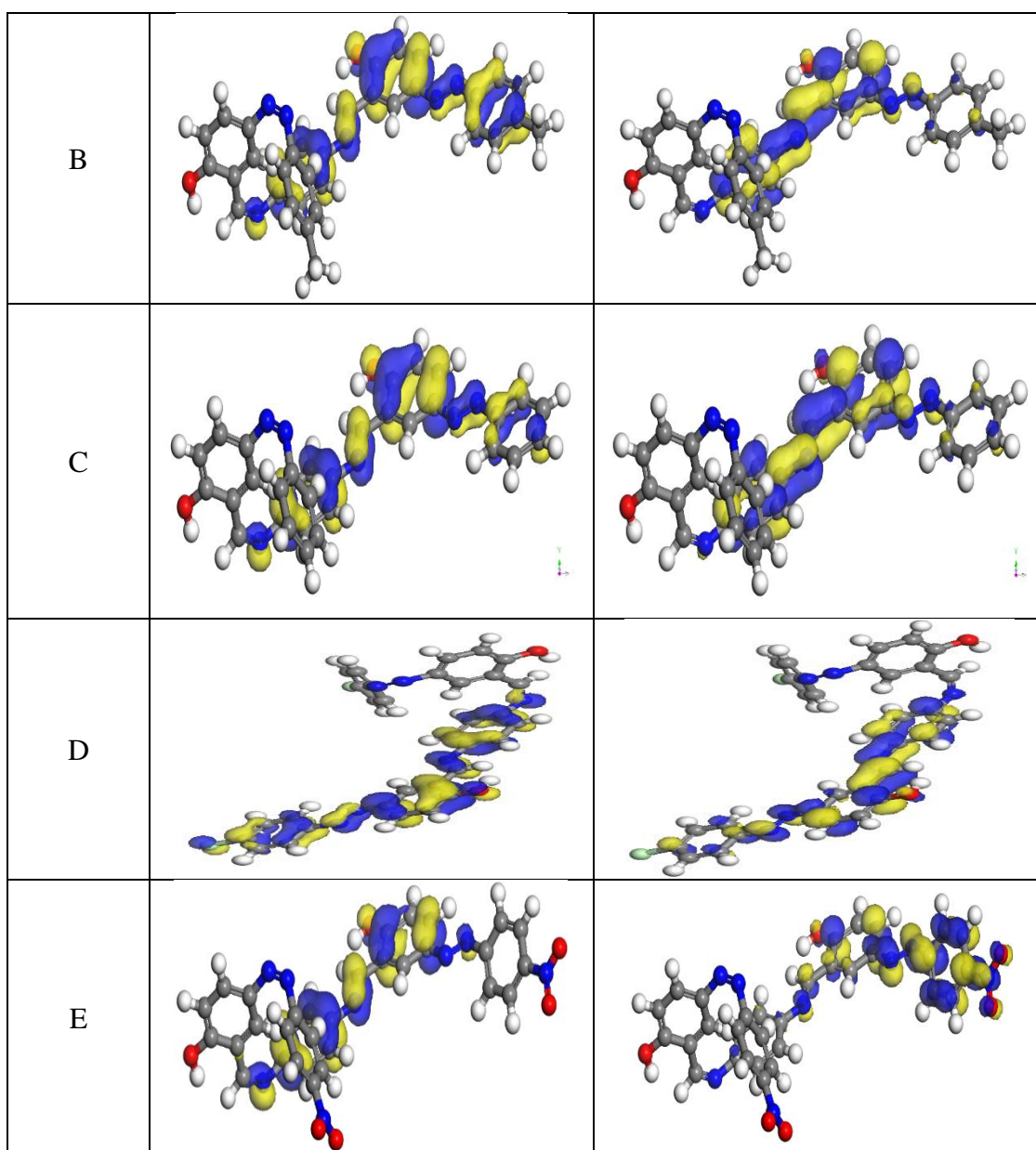


Figure 12. The frontier molecular orbital examined inhibitors (HOMO and LUMO).

Table 9. Parameter obtained from quantum for examined OCs

Inhibitor	$-E_{\text{HOMO}}$ (ev)	$-E_{\text{LUMO}}$ (ev)	ΔE , (ev) ($E_{\text{L}}-E_{\text{H}}$)	μ (Debye)
A	9.187	1.496	7.691	11.500
B	8.858	1.158	7.700	3.756
C	8.833	1.087	7.746	3.344
D	8.819	0.99	7.829	3.281
E	8.799	0.95	7.849	2.233

3.10. Mechanism of inhibition

The protection of α -brass from corrosion in 1M HNO_3 by OCs, utilized all tests, had found to depend on OCs concentration, nature of α -brass, the adsorption mode of the OCs and surface of α -brass settings. These OCs could adsorb in a flat shape among the S, O and N atoms and the kind of groups in para place [43]. %IE lowered with temperature increase, the order of lessening the IE of the OCs in 1.0M HNO_3 was: $A > B > C > D > E$. Linear free energy relationships (LFERs) have been utilized to connect to rate of corrosion without and with OCs with their Hammett constants (σ) yield sign for IE order. The LFER or Hammett balance are obtained by: [44]

$$\text{Log } (k_{\text{rate of corr}}/k^0_{\text{rate of corr}}) = -\rho\sigma \quad (12)$$

Where k^0 and k are the rates of dissolution of α -brass presence and lack of OCs, correspondingly. ρ is the constant reaction σ is the essential in para-position, thus (ρ) is a measure the density of electrons at the reaction site. The +ve sign of σ given electron-withdrawing groups, but -ve sign σ given electron-donating groups. Draw of σ vs. $\text{Log } (\text{rate})$ and the slope equal ρ and its sign designates whether the procedure is protected by improving or lower the electron density. The protection procedures depend on the degree of ρ . Figure 13 display that the OCs give an excellent correlation coefficient (R^2) (0.932). OCs (A) has the higher %IE, because the attendance of $p\text{-OCH}_3$ group which is an electron donating with negative value ($\sigma_{\text{pCH}_3} = -0.27$); $p\text{-OCH}_3$ will improve the electron charge density on the atom. OCs (B) come after (A); due to found $p\text{-CH}_3$ group which is an electron-donating ($\sigma_{\text{CH}_3} = -0.17$), Also this group will increase the density of electron charge on the molecule but with smaller data than $p\text{-OCH}_3$ in (A). OCs (C) with Hammett constant ($\sigma_{\text{H}} = 0.0$) come after compound (B) in %IE, due to $p\text{-H}$ has no effect on the charge density of the compound. As a final point, inhibitor (D) and (E) is the smallest in %IE, because the audience of $p\text{-Cl}$ and $p\text{-NO}_2$ groups which being electron withdrawing ($\sigma_{\text{Cl}} = +0.23$ and $\sigma_{\text{NO}_2} = +0.78$), the relay on the extent of their withdrawing group.

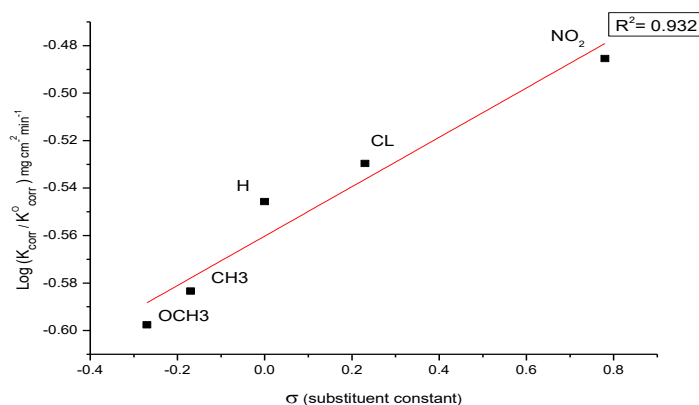


Figure 13. Log k_{corr} versus σ (Hammett constants) of the substituent of OCs

4. CONCLUSIONS

Results obtained from all tests confirmed the organic compounds good inhibition for brass in 1M HNO_3 . There was better corrosion inhibition performance for all the results parameters when the inhibitor concentration was increased. The 21×10^{-6} M organic compound concentration gave the best

corrosion inhibition performance. The reaction of organic compounds with nitric acid provides a stable film that contributed to the passivation of the brass surface to stifle the corrosion process interfacial reactions. A mixed type inhibitor was indicated by the results of β_a and β_c . From the adsorption isotherm results, an inhibitor protection mechanism was a Langmuir isotherm model.

References

1. N. A. Al-Mobarak, K. F. Khaled, N. H. M. Hamed, K. M. Abdel- Azim, N. S. Abdelshafi, *Arabian Journal of Chemistry*, 3(2010)233.
2. A. S. Fouda, H. A. Wahed, *Arab. J. Chem.*, 9 (2016) S91
3. N. Zulfareen, K. Kannan, T. Venugopal, S. Gnanavel, *Arabian Journal of Chemistry*, 9 (2016)121
4. U.R. Evans, *The Corrosion and Oxidation of Metals*, Arnold, London, 1960, p. 324.
5. M. M. Motawe, A.El-Hossiany, A. S. Fouda, *Int. J. Electrochem. Sci.*, 14(2019)1372
6. X. Zhang, W. Jiang, H. Wang, C. Hao, *Journal of Adhesion Science and Technology*, 33(7) (2019) 736
7. R. Ravichandran, N. Rajendran, *Appl. Surf. Sci.*, 241 (2005) 449.
8. R. Ouache, H. Harkat, P. Pale, K. Oulmi, *Natural Product Research*, 33(9) 2019 1374
9. A. A. Fadda, E. M. Afsah, R. S Awad, *European Journal of Medicinal Chemistry*, 60(2013)421
10. H. Ma, S. Chen, L. Niu, S. Zhao, S. Li, D. Li, *J. Appl. Electrochem.*, 32(2002) 65.
11. R. W. Bosch, J. Hubrecht, W. F. Bogaerts, and B. C. Syrett, *Corrosion*, 57(2001)60.
12. S. S. Abdel-Rehim, K. F. Khaled, N. S. Abd-Elshafi, *Electrochim. Acta*, 51 (2006) 3269.
13. Z. Khiati, A.A. Othman, M. Sanchez-Moreno, M. C. Bernard, S. Joiret, E.M.M Sutter, V. Vivier, *Corros. Sci.*, 35 (2011) 3092.
14. W.H. Smyrl, J.O.M. Bockris, B.E. Conway, E. Yeager, R.E. White (Eds.), *Comprehensive Treatise of Electrochemistry*, Plenum Press, New York, 4(1981) 116.
15. M. El Achouri, S. Kertit, H.M. Gouttaya, B. Nciri, Y. Bensouda, L. Pere, M. R Infante, K. Elkacemi, *Prog. Org. Coat.*, 43(2001) 267–273.
16. J.R. Macdonald, W.B. Johanson, J.R. Macdonald (Ed.), *John Wiley & Sons, Fundamentals of impedance spectroscopy*, book chapter 1, New York (1987) 1.
17. S. F. Mertens, C. Xhoffer, B. C. Decooman, E. Temmerman, *Corrosion*, 53 (1997) 381.
18. M. Lagrenée, B. Mernari, M. Bouanis, M. Traisnel, and F. Bentiss, *Corros. Sci.*, 44 (2002) 573.
19. F. Bentiss, M. Lagrenée, and M. Traisnel, *Corrosion*, 56 (2000) 733.
20. E. Kus, F. Mansfeld, *Corros. Sci.*, 48 (2006) 965–979.
21. D. Q. Zhang, Q. R. Cai, X. M. He, L. X. Gao, and G. S. Kim, *Mater. Chem. Phys.*, 114(2009) 612.
22. G. TrabANELLI, in “Corrosion Mechanisms” (Ed. F. Mansfeld) Marcel Dekker, New York, (1987) 119.
23. A.S. Fouda, A. Abd El-Aal, A.B. Kandil, *Desalination*, 201 (2006) 216.
24. F.H. Asaf, M. Abou- Krishna, M. Khodari, F. EL-Cheihk, A. A. Hussien, *Mater. Chem. Phys.*, 93 (2002) 1.
25. A. Fiala, A. Chibani, A. Darchen, A. Boulkamh, K. Djebbar, *Appl. Surf. Sci.*, 253(2007)9347.
26. S. T. Arab and E. A. Noor, *Corrosion*, 49(1993) 122.
27. W. Durnie, R.D. Marco, A. Jefferson, B. Kinsella, *J. Electrochem. Soc.*, 146(1999) 1751.
28. M. K. Gomma and M. H. Wahdan; *Mater. Chem. Phys.*, 39 (1995) 209.
29. E. Khamis, *Corrosion*, 46(1990)476.
30. A. S Fouda, A.M. El-desoky, A.Nabih, *Advances in Materials and Corrosion*, 2 (2013)9.
31. A. N. Frumkin, *Zeitschrift für Physikalische Chemie*, 116 (1925) 466.
32. F. Bensajjay, S. Alehyen, M. El Achouri, S. Kertit, *Anti-Corros. Meth. Mater.*, 50 (2003) 402.
33. L.Tang, X.Li, Y.Si, G.Mu and G.Liu, *Mater. Chem. Phys.*, 95 (2006) 29.

34. A. K.Maayta and N. A. F. Al-Rawashdeh, *Corros. Sci.*, 46 (2004)1129.
35. S.S. Abd El-Rehim, S.A.M. Refaey, F. Taha, M.B. Saleh, R.A. Ahmed, *J. Appl. Electrochem.*, 31 (2001) 429.
36. A. S. Fouda, D. Mekkiaand A. H. Badr, *J.Korean Chem. Soc.*, 57(2013) 264.
37. X. Li and G. Mu, *Appl. Surf. Sci.*, 252 (2005) 1254.
38. G.Mu, X. Li and G.Liu, *Corros. Sci.*, 47 (2005) 1932.
39. B. Wang, M. Du, J. Zang and C.J, Gao, *Corros. Sci.*, 53 (2011) 353.
40. S. Rajendran, C. Thangavelu and G. Annamalai, *J.Chem. Pharm.l Res.*, 4 (2012) 4836.
41. J.M.Costa, J.M.Lluch,*J. Corros.Sci.*, 24 (1984) 929-933.
42. C. Lee, W. Yang and R. G. Parr, *Phys. Rev. B*, 37 (1988) 785-789.
43. L. R. Chauhan and G. Gunasekaran, *Corros. Sci.*, 49 (2007) 1143.
44. H. Ashassi-Sorkhabi, B. Shaabani, and D. Seifzadeh, *Appl. Surf. Sci.*, 239(2005)154.

© 2020 The Authors. Published by ESG (www.electrochemsci.org). This article is an open access article distributed under the terms and conditions of the Creative Commons Attribution license (<http://creativecommons.org/licenses/by/4.0/>).